RSC Advances

PAPER

Cite this: *RSC Adv.*, 2015, **5**, 79022

Preparation of modified cotton cellulose in ionic liquid and its adsorption of Cu(II) and Ni(II) from aqueous solutions

Lei Xu, Xiaoqiong Lu and Xiaomin Cheng*

A series of novel cotton cellulose-*graft*-polycaprolactone copolymers with different grafting contents were successfully prepared *via* ring-opening polymerization (ROP) in an ionic liquid 1-*N*-butyl-3-methylimidazolium chloride ([Bmim]Cl). The structures of the grafting copolymers were systematically characterized by FTIR, CP/MAS^{13}C-NMR, XRD, SEM and AFM, while thermal properties were investigated by DSC and TGA. Subsequently, Langmuir, Freundlich, Temkin, and Dubinin–Radushkevich (D–R) adsorption isotherms were representative to simulate adsorption isotherms of Cu(II) and Ni(II) ions in aqueous solution. From the comparison of different adsorption isotherm models, it was found that adsorption of Cu(II) by modified cellulose followed Langmuir, Freundlich and Temkin models, while that of Ni(II) followed the Freundlich model. The results of adsorption indicated that the selectivity sequence of metal ions on graft copolymers was Cu(II) > Ni(II) and the maximum removal capacities of Cu(II) and Ni(II) ions were 98.7% and 35.6%, respectively. Hence, the graft copolymers exhibited significant potential to be an environmentally feasible biosorbent for removal of Cu(II) and Ni(II) ions from aqueous solution.

Received 5th May 2015
Accepted 7th September 2015

DOI: 10.1039/c5ra08265j

www.rsc.org/advances

Introduction

Nowadays environmental awareness and the demand for green technology have led to a rapidly increasing interest in biomass resources. Cellulose, with a repeating structure unit of β-(1 → 4)-D-glucose, is the most abundant natural biomaterial in nature, as well as having very attractive advantages such as being inexpensive, renewable and biodegradable, *etc.*[1,2] However, its applications are still limited due to its intrinsic disadvantages. With the increasing demand to use cellulose more effectively, modification of cellulose by graft polymerization provides a significant route to combine the advantages of natural and synthetic macromolecules for a wide range of potential applications such as temperature responsiveness, hydrophobicity and adsorption, *etc.*[3,4]

In the past years, much attention has been paid to the graft polymerization of monomers onto cellulose.[5–10] Lönnberg *et al.* reported surface grafting of microfibrillated cellulose (MFC) with poly(ε-caprolactone) *via* ring-opening polymerization (ROP) to enable dispersion of MFC in nonpolar organic solvents, or in hydrophobic polymeric matrices.[5] Hokkanen *et al.* studied the adsorption properties of aminopropyltriethoxysilane (APS) modified microfibrillated cellulose (MFC) in aqueous solutions containing Ni(II), Cu(II) and Cd(II) ions.[6] Various synthetic polymers such as poly(methacylic acid-*co*-maleic acid)[7] and poly(glycidyl methacrylate)[8,9] have also been grafted onto cellulose or cellulose derivatives. In previous studies, nanofibrillated cellulose (NFC), microfibrillated cellulose (MFC) or regenerated cellulose were selected as the sources of cellulose. However, the potential of cellulose has not yet been completely exploited due to the limited number of common solvents that readily dissolve cellulose.

Since Swatloski *et al.* firstly reported the use of an ionic liquid as solvent media for cellulose, an environmental-friendly reaction scheme for cellulose modifications became practicable under homogeneous solution conditions.[11] Compared with heterogeneous reaction, the advantages of the homogeneous reaction in ionic liquid include: opening new avenues for the design of grafting copolymers, opening up the opportunity to control the degree of substitution and physicochemical property of products, *etc.*[12,13] Many studies have been carried out to use ionic liquids as reaction media for the homogeneous functionalization of different cellulose.[14–22] For example, poly(*N*-isopropylacrylamide),[14] poly(*p*-dioxanone)[18] and poly(methylmethacrylate)[19] were successively reported to be grafted on cellulose or cellulose derivatives in ionic liquid.

An important application of modified cellulose is used for adsorbent. Maater[7] reported a poly(methacrylic acid-*co*-maleic acid) grafted nanofibrillated cellulose (NFC-MAA-MA) aerogel *via* radical polymerization in an aqueous solution using Fenton's reagent, which showed an efficient adsorption, exceeding 95% toward Pb^{2+}, Cd^{2+}, Zn^{2+} and Ni^{2+}. Lin *et al.*[22] successfully prepared glycidyl methacrylate grafted cellulose and used them as good sorbents for metal ions. The products showed more

School of Chemistry and Chemical Engineering of Anhui University & Key Laboratory of Environment-friendly Polymer Materials of Anhui Province, Hefei 230601, China. E-mail: xmcheng@adu.edu.cn

effective adsorption of Cr(VI) ions than other adsorbents reported in the literature. Another biosorbent, developed by chemically modifying the *Moringa oleifera* leaves powder by esterifying with NaOH followed by citric acid treatment, were reported by Kumar Reddy.[23] The modified biosorbent could be used for the removal of Cd(II), Cu(II) and Ni(II) from aqueous solution. Yu and coworkers[24] deposited $CoFe_2O_4$ nanoparticles on cellulose beads to obtain porous magnetic cellulose beads for the removal of metal ions. The encapsulated $CoFe_2O_4$ nanoparticles act as the magnetic substrate and the active sites to adsorb metal ions.

In our work, cotton cellulose, a semi-product of cotton-plant with α-cellulose as the major component was used as the raw material to prepare cellulose-*g*-PCL copolymers *via* ring opening polymerization (ROP) in an ionic liquid 1-*N*-butyl-3-methylimidazolium chloride ([Bmim]Cl). Poly(ε-caprolactone) (PCL) is an important aliphatic polyesters with good biocompatibility, mechanical and biodegradability and has been used in many fields, such as biological medicine, adsorption, *etc.*[25,26] Although the grafting of PCL on cellulose has been studied in various system,[5,10,16] biodegradable adsorbent prepared in ionic liquid [Bmim]Cl based on cotton cellulose and PCL as we report in this work was observed for the first time to the best of our knowledge. In order to well understand the copolymers, the resultant copolymers were systematically characterized by FT-IR, CP/MAS^{13}C-NMR, XRD SEM and AFM. Their thermal property was studied by DSC and TGA. In addition, the adsorption behaviors of cellulose-*g*-PCL copolymers for Cu(II) and Ni(II) ions were carefully studied. Langmuir, Freundlich, Temkin, and Dubinin–Radushkevich (D–R) adsorption isotherms were used to simulate adsorption isotherms of Cu(II) and Ni(II) ions. The efficiency of this modified cellulose material in removal of Cu(II) ions from aqueous solutions is very promising.

Experimental

Materials

The cotton cellulose substrate, degreasing cotton (purchased from Winner Medical Group Co., Shenzhen, China) was vacuum dried at 70 °C for 24 h before use. The ionic liquid, 1-*N*-butyl-3-methylimidazolium chloride ([Bmim]Cl) (99.0%) (Lihua Pharmaceutical Co., Ltd, Henan, China) was dried in vacuum for 48 h at 45 °C before use. The monomer ε-caprolactone (ε-CL, 99%, Aladdin) was purified by reduced pressure distillation over CaH_2. Tin 2-ethylhexanoate ($Sn(Oct)_2$, Aladdin, 95%) was used as received without further purification. Other solvents were of analytical reagent grade and directly used without further purification.

Characterization

The FT-IR spectra of cellulose and copolymers were recorded using a Nicolet NEXUS-870 FTIR spectrometer. The solid CP/MAS^{13}C-NMR spectrum of copolymer was recorded on a Bruker AV 400 M spectrometer. XRD of samples was determined by a MXP18AHF X-ray diffractometer, in which the high-intensity monochromatic nickel-filtered CuKα radiation was generated at 40 kV and 100 mA. Samples were scanned at a speed of 4° min^{-1} and a step size of 0.04° in the range of 2θ = 5–50° at room temperature. DSC measurements were conducted using a Q2000 DSC (TA Instruments). Samples of about 4 mg were first heated from 25 °C to 200 °C with a heating rate of 20 °C min^{-1} under nitrogen atmosphere and held for 3 min to erase the thermal history, then cooled rapidly to −70 °C, and finally heated to 200 °C at 20 °C min^{-1}. TGA measurements were carried out on a 449F3 thermogravimetric analyzer (Netzsch Co.). Samples of approximately 6 mg weight were heated in an aluminum crucible to 700 °C at a heating rate of 20 °C min^{-1} while the apparatus was continually flushed with a nitrogen flow of 30 mL min^{-1}. SEM samples were prepared by putting the sample power on a slide plate. After gold-plating, the samples were observed by S-4800 scanning electron microscope (Hitachi). AFM images of the polymers were performed using a CSPM500 atomic force microscope (BenYuan Ltd). Samples were prepared according to the following procedure: 2.0 mg cellulose powder or cellulose-*g*-PCL copolymer powder was placed into 20 mL acetone, and then dispersed in ultrasonic bath for certain time to obtain a uniform and transparent solution. The same amount of two solutions was dropped to newly fresh micas. Subsequently these micas were self-dried at room temperature.

The absorption capacity of copolymers was evaluated by a batch method. Two solutions of Cu(II) and Ni(II) ions were prepared from analytical-grade copper(II) sulfate and nickel(II) sulfate, respectively. Sorption experiments were conducted in a conical flask and equilibrated using a shaker. Then, 50, 100, 200, 300, 400 and 500 mg L^{-1} of each of these solutions were separately placed in flasks and equilibrated with a certain samples at room temperature. After a certain time of shaking, the solutions were filtered, and the filtrates were analyzed using a M6-5000 atomic absorption spectrometer (AAS, TA).

The adsorption capacity q_e (mg g^{-1}) was calculated as described by the following eqn (1):

$$q_e = \frac{(C_0 - C_e)V}{W} \quad (1)$$

where C_0 (mg L^{-1}) is the initial metal ion concentration, C_e (mg L^{-1}) is the equilibrium concentration of metal ion, V (L) is the volume of the metal ion solution, and W (g) is the weight of adsorbent.

The removal efficiency (R%) of the adsorbent was calculated with the following formula:

$$R(\%) = \frac{(C_0 - C_e)}{C_0} \times 100 \quad (2)$$

Synthesis of copolymers

A typical polymerization procedure was shown as follows: 0.5 g cotton cellulose was added to 15 g [Bmim]Cl in a 100 mL dried three-neck flask. The mixture was vigorously stirred at 100 °C for 10 h under nitrogen to gain a homogeneous solution. Then the monomer of ε-CL and a catalytic amount of $Sn(Oct)_2$ were added into the polymerization flask. The flask was connected to a Schlenk line, where exhausting-refilling processes were

repeated 3 times. Finally, the flask was immersed into an oil bath at 120 °C under nitrogen atmosphere with vigorous stirring for a certain time. After cooling to room temperature, the resultant polymers were precipitated with ethanol and washed for several times. Subsequently, the resultant polymers were extracted *via* Soxhlet extraction for 72 h with dichloromethane. The purified copolymers were dried in a vacuum oven until constant weight. The graft ratio (%) was calculated by eqn (3):

$$\text{graft ratio}(\%) = \frac{W_{\text{graft}} - W_{\text{cell}}}{W_{\text{cell}}} \times 100 \quad (3)$$

where W_{cell} and W_{graft} are the dry weight of native cellulose and copolymers, respectively.

Table 1 Reaction conditions of cellulose-*g*-PCL copolymers

Samples	ε-CL/cell (g g^{-1})	Catalysts (wt%)	Reaction time (h)	Yield (g)	GR (%)
C1	8 : 1	0.5	18	0.554	10.8
C2	10 : 1	0.5	18	0.585	16.9
C3	15 : 1	0.5	18	0.662	32.4
C4	20 : 1	0.5	18	0.607	21.3
C5	15 : 1	0.2	18	0.564	12.7
C6	15 : 1	1.0	18	0.573	14.6
C7	15 : 1	0.5	12	0.536	7.2
C8	15 : 1	0.5	24	0.577	15.3

Results and discussion

Synthesis of copolymers

A series of cotton cellulose-*g*-PCL copolymers were synthesized *via* homogeneous ring-opening polymerization (ROP) of ε-CL onto cellulose in ionic liquid [Bmim]Cl using $Sn(Oct)_2$ as the catalyst, and the polymerization procedure was displayed in Scheme 1. The ionic liquid [Bmim]Cl, a powerful solvent for biomass, was selected to make the ROP reaction performed in a homogeneous environment and can reduce pollution for environment. By controlling the mass ratio of cellulose and ε-CL, the amount of $Sn(Oct)_2$ and reaction time, the copolymers with various grafting content can be obtained. The results of the graft copolymerization under various reaction conditions are summarized in Table 1.

It could be found that the grafting content of copolymers increased with the increasing mass ratio of CL/cell (g g^{-1}) up to 15/1, then decreased with further increasing the mass ratio of CL/Cell (g g^{-1}). This trend could be explained as that probability of collision and reaction between ε-CL monomers and anhydrous glucose units (AGU) units increased when more ε-CL monomers were introduced. With the further increasing monomers dosage, the concentration of active groups also increased in favor of the collision between ε-CL monomers and active groups, thus decreasing the grafting content of grafting polymers. Another tendency was that the grafting content of copolymers varied with catalysts dosages. The grafting content of copolymers increased with increasing the amount of $Sn(Oct)_2$ up to 0.5 wt% of ε-CL monomers, and then decreased. With further increasing catalysts dosage, the speed of the chain transfer and termination can increase, thus decreasing the grafting ratio of copolymers. In addition, the grafting content of copolymers increased with reaction time up to 18 h then decreased. With further increasing reaction time, polymers of reactive system can be thermal decomposition under high temperature, so the grafting content of copolymers also decreased. However, all samples had poor solubility in organic solvent or water due to the limited graft ratio.

FTIR and CP/MAS^{13}C-NMR analysis

To attest that the signal at 1732 cm^{-1} was just from the PCL segments of cellulose-*g*-PCL copolymers, but not homo-PCL or ε-CL mixed with cellulose, a sample of regenerated cellulose (reg-cellulose) was prepared by stirring a mixture of cotton cellulose, the homo-PCL and ε-CL in [Bmim]Cl at 120 °C for 18 h. Subsequently, the homo-PCL and the ε-CL monomers were

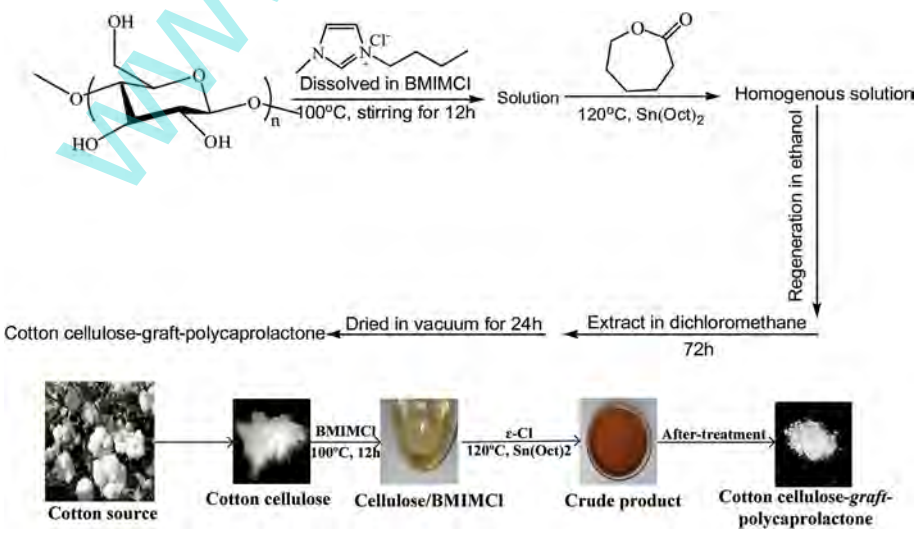

Scheme 1 The grafting copolymerization of PCL onto cotton cellulose backbone in ionic liquid [Bmim]Cl.

removed by Soxhlet extraction with dichloromethane for 72 h. Fig. 1A illustrates that the FTIR spectra of reg-cellulose and mixture of cellulose and PCL. The result showed that the signal at 1732 cm^{-1} completely disappeared after extraction, indicating that all mixed homo-PCL and ε-CL monomer can be removed by extraction with dichloromethane within 72 h.

The FT-IR spectra of cellulose and cellulose-*g*-PCL copolymers with various graft contents were displayed in Fig. 1B. From the result of extraction, the peak at 1732 cm^{-1} of Fig. 1B was just from the PCL segments of copolymers. In the FTIR spectrum of cellulose, the peak in the range of 3000–3500 cm^{-1} was assigned to the –OH stretching, the characteristic peak at 1161 cm^{-1} was attributed to the asymmetric C–O stretching of –C–O–C bridge, the peak 899 cm^{-1} was assigned to the C–O stretching of glycoside linkage and the peak at 1643 cm^{-1} belonged to the C–H stretching of CH_2 groups. For the FTIR spectrums of copolymers (C3, 4, 6, 7), the characteristic peaks at 1732 cm^{-1} were assigned to the stretching vibration of C=O of PCL ester group, and the intensity of the peaks enhanced with increasing the grafting ratio of copolymers. The results showed that PCL parts were grafted onto cellulose.

The CP/MAS^{13}C-NMR spectrum of cotton cellulose-*g*-PCL copolymer was shown in Fig. 1C. The carbonyl carbon signal Ca of the PCL segments in copolymer appeared at $\delta = 174.1$ ppm, and the methylene carbon signals of the PCL segments also could be observed at $\delta = 62$ ppm, 34 ppm, and 25 ppm, corresponding to Cf, Cb and Ce, Cc and Cd positions, respectively. The carbon signals of the cellulose backbone appeared at $\delta = 105.4$ ppm, 88.6 ppm, 71–75 ppm and 64.6 ppm, assigned to C1, C4, C235, and C6 of anhydrous glucose units (AGU), respectively. Compared with the CP/MAS^{13}C-NMR spectrum of pure reg-cellulose, the carbon location of anhydrous glucose units in copolymers appeared drifting. Moreover, the carbon signal located at $\delta = 97.8$ ppm (C1′) belonged to the C1 adjacent to the C2 with substituted –OH groups, which was cleaved from signal from C1 by the affection of groups in PCL chains. The results further indicated the PCL chains were grafted onto cellulose.

X-ray diffraction (XRD)

The XRD patterns of PCL and cellulose-*g*-PCL copolymers were presented in Fig. 2. The XRD pattern of PCL showed two main

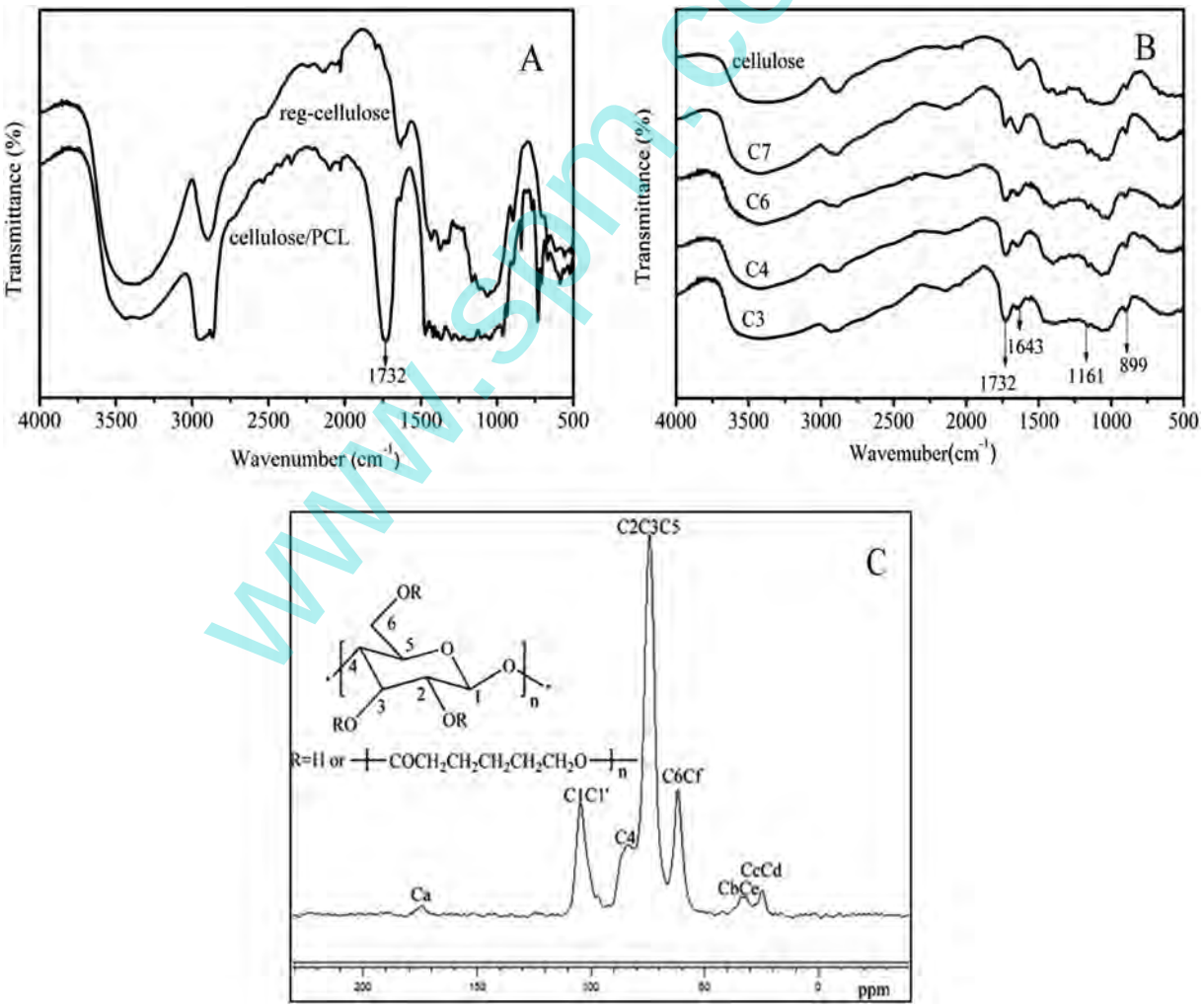

Fig. 1 FTIR spectra (A and B) of samples and CP/MAS^{13}C-NMR (C) spectrum of cellulose-*g*-PCL copolymer.

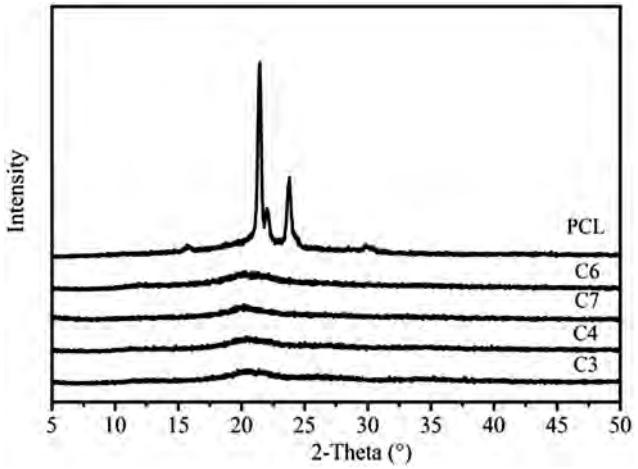

Fig. 2 XRD patterns of PCL and cellulose-*g*-PCL copolymers (C3, C4, C6, C7).

diffraction peaks at $2\theta = 21.4°$and 23.8°, corresponding to the diffraction planes of (110) and (200), respectively. Some previous literatures have reported that native cellulose has three peaks at $2\theta = 15.2°$, 16.7°, and 23.1°, and its reg-cellulose also has one peak at $2\theta = 22.4°$.[27] However, in the paper, the patterns of cellulose-*g*-PCL copolymers didn't showed the crystallization peaks of PCL and cellulose. On the other hand, a dispersive broad peak in the range of 18–22° appeared in the diffraction patterns of copolymers, indicating that the PCL chains of copolymers just possessed partial ordering structure due to the limited length of PCL chains. The results suggested that the original crystalline structures of cellulose could be disrupted by the introduction of PCL parts.

Thermodynamic analysis

The DSC thermograms of PCL and cellulose-*g*-PCL copolymers were shown in Fig. 3A and B. It was well regarded that the native cellulose didn't show obvious glass transition temperature (T_g) and melting temperature (T_m) in the range of heating scan due

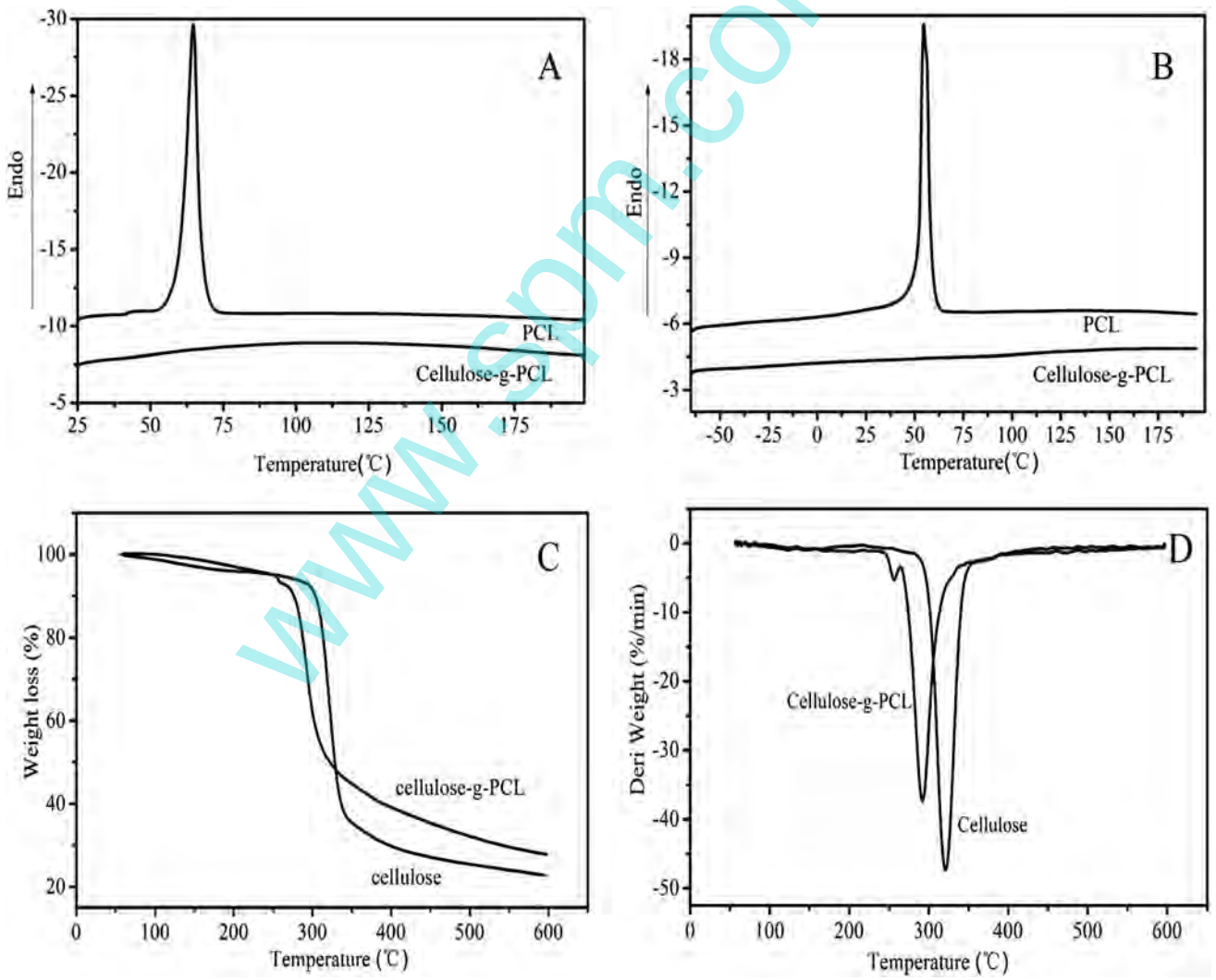

Fig. 3 DSC thermograms ((A): first heating runs; (B): second heating runs), TGA curves (C) and DTG curves (D) of PCL and cotton cellulose-g-PCL copolymer.

to the strong inter- and intra-hydrogen bonds. In the first and second heating runs of pure PCL, the melting peaks of PCL were detected at 60 °C and 54 °C, respectively. However, the melting peak of PCL chains was not observed in the DSC thermograms of copolymer. The results suggested PCL side chains of copolymers have very poor crystal structure. It may be original from the fact that the chain length of PCL segments was limited. Furthermore, the crystallization of PCL side chains may be greatly restrained by cellulose main chains. This result was consistent with that obtained by XRD measurement.

The TGA and DTG curves for both cellulose and copolymer at a heating rate of 20 °C min^{-1} under nitrogen atmosphere were displayed in Fig. 4C and D. It can be found that cellulose went through a stage of thermal degradation from 60 °C to 200 °C with a slight weight loss about 4% owing to the vaporization of water or elimination of unstable fragments. Subsequently, a weight loss started from 240 °C to 431 °C due to the degradation of cellulose main chains. And the maximum degradation rate of cellulose could be recorded at the temperature of 321 °C. In contrast with cellulose, the thermal degradation of cellulose-*g*-PCL copolymers exhibited two separated pyrolysis. The first process extending from 230 °C to 265 °C was possibly ascribed to the degradation of cellulose fragments, and the second process starting from 265 °C to 406 °C should be corresponded to the degradation of copolymers. Moreover, a maximum degradation rate could be observed at the temperature of 293 °C from the TG and DTG curves. Furthermore, we can find that the onset decomposition temperature and the maximum decomposition temperatures of copolymers were lower than those of cellulose. The results could be attributed to the fact that the introduction of PCL parts partially destroyed the hydrogen bonds of cotton cellulose, thereby affected the crystalline structure of cellulose.

Morphology of cellulose and cellulose-*g*-PCL copolymer

SEM images of cellulose and cellulose-*g*-PCL copolymer were presented in Fig. 4A and B. Both images showed the clear cut difference on the surface morphology of the cellulose and copolymer. The surface of cellulose showed a comparatively smooth, continuous and dense topography with many ridges situated parallel to each other. However, the surface of copolymer showed a relatively rough and flat morphology with many obvious pores compared to the surface of reg-cellulose. It can be explained as that the crystalline regions of cellulose were interrupted by the introduction of PCL parts.

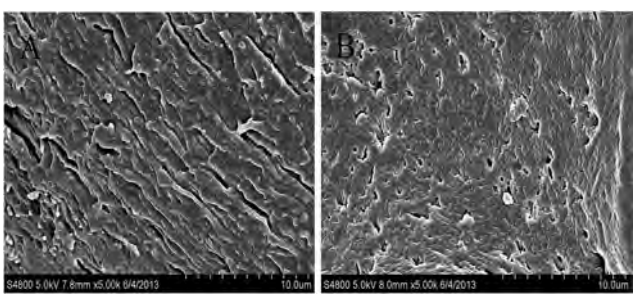

Fig. 4 SEM images of cellulose (A) and graft copolymer (B).

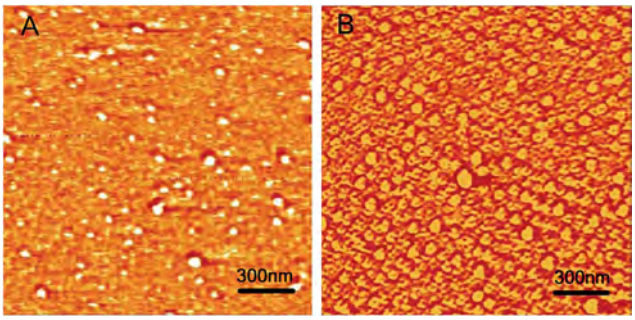

Fig. 5 AFM images of cellulose powders (A) and copolymer powders (B).

The distribution characterizations of cellulose and copolymer powders in acetone were examined by AFM, as displayed in Fig. 5A and B. The particles of cellulose and copolymer showed a kind of grain shape. Fig. 5A showed that cellulose samples had a good dispersion in acetone, and the size of particles was comparatively non-uniform. However, in Fig. 5B, the copolymer particles had a relatively dense distribution as well as orderly arrangement, and the size of particles was relatively uniform. From AFM measurement, it can be seen that the average diameter (28.1 nm) of copolymer particles was smaller than (32.2 nm) that of cellulose, and the roughness average value ($R_a = 0.709$ nm) of copolymer sample was higher than that ($R_a = 0.436$ nm) of cellulose. The results may be because that the surface property of cellulose was changed by grafting PCL chains.

Adsorption studies and isotherms

The equilibrium adsorption isotherm is fundamental method to describe the interactive behavior between the adsorbate and adsorbent, and the relationship between the concentration of adsorbent and dissolved adsorbate at equilibrium. The results of adsorption can be analyzed using different isotherm equations, such as Langmuir, Freundlich, Dubinin–Radushkevich and Temkin isotherm equations.

The Langmuir model is often applied to assume the occurrence of adsorption at specific homogeneous adsorption sites within the adsorbent.[28] The linear form of the Langmuir equation can be written as follows:

$$\frac{C_e}{q_e} = \frac{1}{bQ_0} + \frac{C_e}{Q_0} \quad (4)$$

where b (L g^{-1}) is Langmuir constant and Q_0 (mg g^{-1}) is the maximum amount of the metal ions adsorbed per unit weight of the adsorbent. C_e (mg L^{-1}) and q_e (mg g^{-1}) are the concentration and adsorption capacity at the equilibrium, respectively. The value of b and Q_0 can be obtained from the slope and intercept of a linear plot of C_e/q_e *versus* C_e.

The linear Langmuir adsorption isotherms of Cu(II) and Ni(II) ions on copolymers were displayed in Fig. 6A, and isotherm constants were presented in Table 2. For Cu(II) ions, high R^2 values (correlation coefficients) showed that the Langmuir isotherm fit rather well with the experimental data. However, the adsorption of Ni(II) ions on copolymers did not follow

Langmuir model, indicating more complex adsorption phenomena than simple monolayer formation.

The separation constant R_L (dimensionless constant) of Langmuir isotherm, defined by Weber and Chakraborty,[29] can be used to predict the affinity between the adsorbate and adsorbent in the absorption system and represented as follows:

$$R_L = \frac{1}{1 + bC_0} \quad (5)$$

where b (L mg^{-1}) refers to the Langmuir constant and C_0 (mg L^{-1}) is initial concentration of metal ions. The R_L value indicates the nature of absorption to be either unfavorable ($R_L > 1$), linear ($R_L = 1$), favorable ($0 < R_L < 1$), or irreversible ($R_L = 0$).[29] For all selected concentrations (50–500 mg L^{-1}) of Cu(II) ions, the values of R_L ranged from 0.4546 to 0.8929. Consequently, cellulose-*g*-PCL copolymers were found to be the favorable adsorbent for Cu(II) ions.

Another linear equation of the Freundlich adsorption model[30] is

$$\log q_e = \log K + \frac{1}{n} \log C_e \quad (6)$$

where K and n are indicators of adsorption capacity and adsorption intensity, respectively. A plot of log q_e *vs.* log C_e gave a straight line with the slope ($1/n$) and intercept (log K), as shown in Fig. 6B. The higher correlation coefficients indicated that the adsorption of Cu(II) and Ni(II) ions followed the Freundlich model. With the help of slope and intercept, the n and the K values were calculated and listed in Table 2. For the adsorption of Ni(II), the higher correlation coefficient was obtained from Freundlich model when compared to the Langmuir model. This observed result suggests that the adsorption of Ni(II) was taken place on the heterogeneous surface of the adsorbent much better than the monolayer adsorption.

In order to deduce the heterogeneity of the surface energies of adsorption and the characteristic porosity of the adsorbent, the Dubinin–Radushkevich (D–R) isotherm model was further applied to the data of adsorption.[31] The linear form of D–R isotherm model is given as follows:

$$\ln q_e = \ln q_m - \beta\varepsilon^2 \quad (7)$$

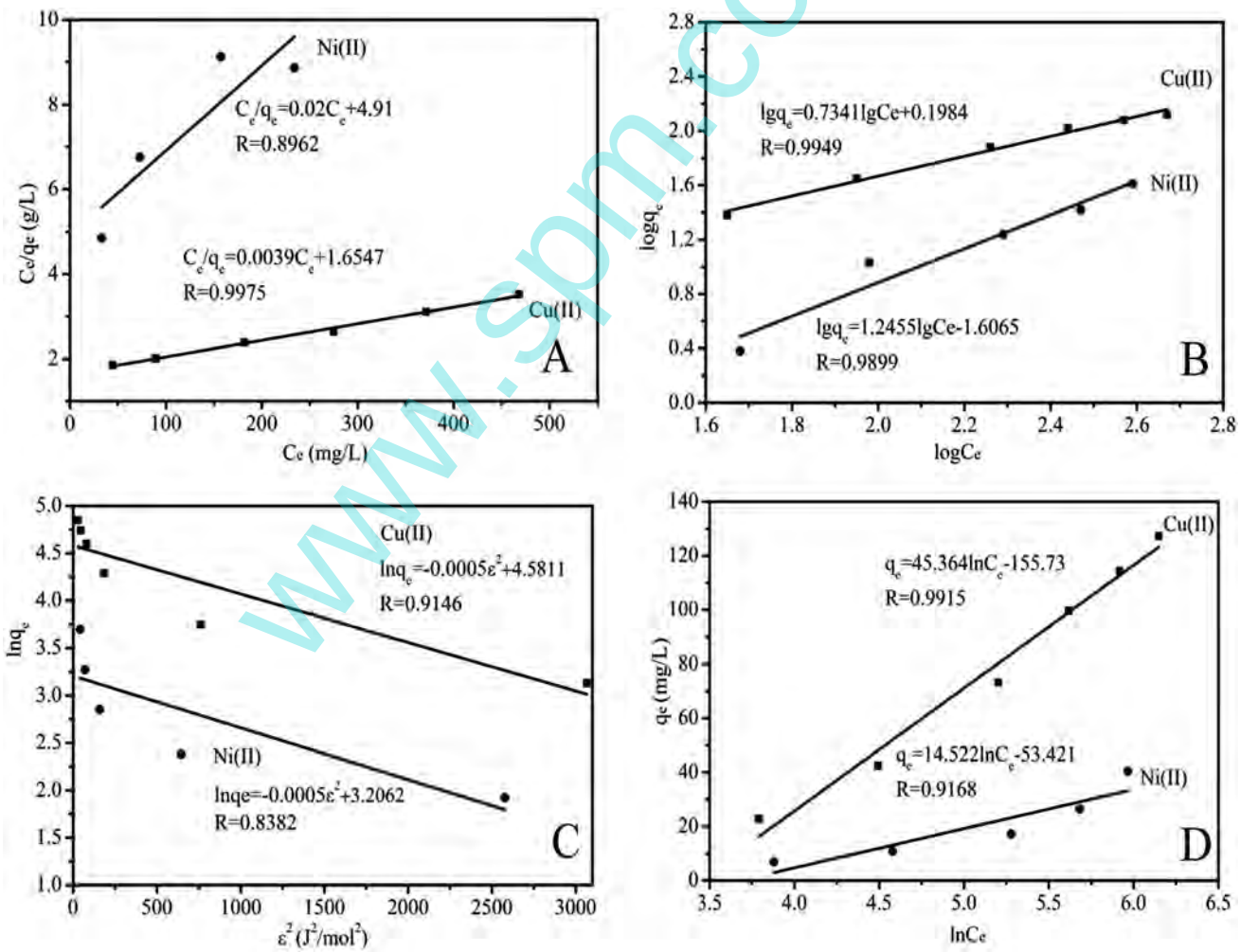

Fig. 6 Langmuir (A), Freundlich (B), Dubinin–Radushkevich (D–R) (C) and Temkin (D) adsorption isotherms for Cu(II) and Ni(II) ions on cellulose-*g*-PCL copolymers.

Table 2 Isotherm constants of cellulose-PCL copolymers for Ni(II) and Cu(II) ions

Type of metal	Q_0 (mg g^{-1})	b (L mg^{-1})	R^2
Langmuir			
Cu(II)	256.4	0.0024	0.9951
Ni(II)	50	0.0041	0.8032

Type of metal	K (L g^{-1})	$1/n$	R^2
Freundlich			
Cu(II)	1.5791	0.7341	0.9898
Ni(II)	0.0248	1.2455	0.9799

Type of metal	q_m (mg g^{-1})	β	E	R^2
D–R				
Cu(II)	97.58	0.0005	0.032	0.8365
Ni(II)	24.68	0.0005	0.032	0.7062

Type of metal	B (mg g^{-1})	K_T	b' (J mol^{-1})	R^2
Temkin				
Cu(II)	45.36	0.0325	54.62	0.9831
Ni(II)	14.52	0.025	170.61	0.8405

where β (kJ^2 mol^{-2}) is D–R constant connected with the mean free energy of adsorption per mole of the adsorbate, and q_m (mg g^{-1}) is the theoretical saturation capacity. ε is the Polanyi potential,[32] which is equal to:

$$\varepsilon = RT \ln\left(1 + \frac{1}{C_e}\right) \quad (8)$$

where T (K) and R (8.3143 J mol^{-1}) are the absolute temperature and the universal gas constant, respectively. The apparent energy (E) of adsorption is calculated as follows:[33]

$$E = \frac{1}{\sqrt{2\beta}} \quad (9)$$

where E (kJ mol^{-1}) is the mean free energy of adsorption per molecule of the adsorbate when transferred to the surface of the solid from infinity in solution.

The (D–R) constants for Cu(II) and Ni(II) ions were calculated from Fig. 6C, and results are given in Table 2. R^2 values of Cu(II) and Ni(II) ions were less than 0.98, hence, the adsorption of Cu(II) and Ni(II) ions on copolymers cannot follow the D–R isotherm model. The E of adsorption was found to be 0.032 kJ mol^{-1}. If the value of E (kJ mol^{-1}) lies between 8 and 16 kJ mol^{-1}, the nature of the sorption process is chemical; the value below 8 kJ mol^{-1} indicates a physical adsorption process.[34] Therefore, the adsorption of Cu(II) and Ni(II) ions was physical in nature. Since the adsorption of Cu(II) and Ni(II) ions did not follow D–R isotherm model, the E values only provided an estimation of nature of adsorption process.

Temkin isotherm assumes that heat of adsorption decreases linearly with the adsorption onto the surface at a particular temperature, and the adsorption is characterized by a uniform distribution of binding energies.[35] Temkin isotherm is expressed in linear form by the following equation:

$$q_e = B \ln K_T + B \ln C_e \quad (10)$$

$$B = \frac{RT}{b'} \quad (11)$$

where B is related to the heat of adsorption, K_T (L mg^{-1}) is the equilibrium binding constant, and b' (J mol^{-1}) indicates the adsorption potential of the adsorbent. The parameters for the Temkin model are obtained from the plot of q_e *versus* ln C_e (Fig. 6D). The R^2 values indicated that the adsorption of Cu(II) ions on copolymers followed Temkin model, while that of Ni(II) ions did not.

From the comparison of various adsorption isotherm models, the adsorption of Cu(II) ions on copolymers followed Langmuir, Freundlich and Temkin isotherm models. For Ni(II) ions, its adsorption only followed Freundlich isotherm model.

As shown in Fig. 7, the removal capacity R decreased with the increase of initial concentration (C_0) of Cu(II) and Ni(II) ions. This may be because the adsorption sites and space of copolymer were limited. In addition, when C_0 was 50 mg L^{-1}, the maximum R values of Cu(II) ions and Ni(II) ions were 98.7% and 35.6%, respectively. For all selected concentrations (50–500 mg L^{-1}), R value of Cu(II) ions was higher than that of Ni(II) ions. This suggested that the selectivity sequence of cellulose-*g*-PCL copolymers for metal ions was Cu(II) > Ni(II). Hajeeth *et al.*[36] investigated the adsorption of cellulose-*g*-acrylic acid for Cu(II) and Ni(II) ions, and the removal capacity of Cu(II) ions (78.2%) was higher than that of Ni(II) ions (57.3%). O'Connell *et al.*[8,9] studied the adsorption of cellulose-*g*-GMA-imidazole for Cu(II) and Ni(II) ions, and the removal capacity of Cu(II) ions was also higher than that of Ni(II) ions. These results were similar to that of cellulose-*g*-PCL copolymers. However, the adsorption data of metal ions on aminopropyltriethoxysilane modified microfibrillated cellulose (Hokkanen *et al.*[6]) and cellulose-*g*-α-thioglycerol (Aoki *et al.*[37]) showed a opposite selectivity sequence, Ni(II) > Cu(II). It is possible that introducing different grafting

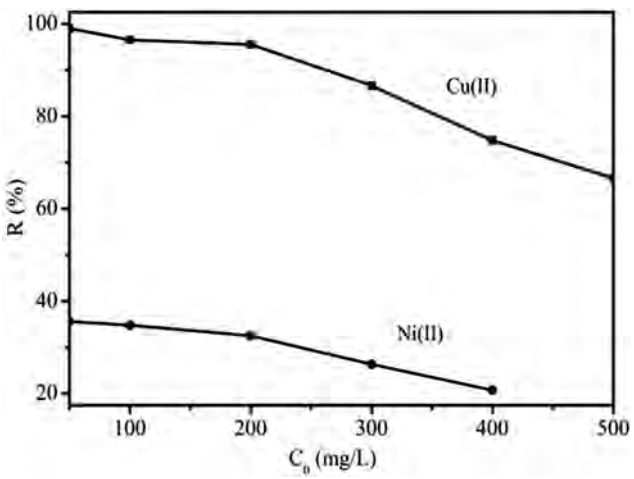

Fig. 7 Removal capacity R of Cu(II) and Ni(II) ions as a function of initial concentration (C_0).

groups plays an important role in the adsorption of cellulose for metal ions.

Conclusions

In summary, a modified cellulose was successfully synthesized *via* homogeneous ROP of ε-CL onto cotton cellulose backbone in ionic liquid [Bmim]Cl, which was verified by the FTIR and CP/MAS ^{13}C NMR analysis. The graft copolymers were amorphous and their thermal stability was lower than that of cellulose. SEM and AFM observation illustrated that the modified cellulose surfaces became much rougher due to the presence of grafting PCL chains. The adsorption of Cu(II) agreed well with Langmuir isotherm, Freundlich and Temkin isotherm models, and the biosorbent (cellulose-*g*-PCL) exhibited satisfactory removal capacity of 98.7% for Cu(II) ions in aqueous solution. The adsorption of Ni(II) only followed Freundlich isotherm model and the removal capacity of Ni(II) ions was 35.6%. This study demonstrates that green synthesis of cellulose-*g*-PCL is an effective pathway to obtain satisfactory biosorbent for the removal of Cu(II) and Ni(II) ions from aqueous solution.

Acknowledgements

We thank for help with Key Laboratory of Environment-friendly Polymer Materials of Anhui Province and the innovation team project of advance functional materials supported by Ministry of Education in China.

References

1 D. Klemm, B. Heublein, H. P. Fink and A. Bohn, *Angew. Chem., Int. Ed.*, 2005, **44**(22), 3358–3364.
2 D. Roy, M. Semsarilar, J. T. Guthrie and S. Perrier, *Chem. Soc. Rev.*, 2009, **38**(7), 2046–2054.
3 M. Isik, H. Sardon and D. Mecerreyes, *Int. J. Mol. Sci.*, 2014, **15**, 11922–11934.
4 G. S. Chausan, S. Mahajan and L. K. Guleria, *Desalination*, 2000, **130**, 85–98.
5 H. Lönnberg, L. Fogelström, E. Malmström and A. Hult, *Eur. Polym. J.*, 2008, **44**, 2991–3014.
6 S. Hokkanen, E. Repo, T. Suopajärvi, H. Liimatainen, J. Niinimaa and M. Sillanpää, *Cellulose*, 2014, **21**, 1471–1483.
7 W. Maatar and S. Boufi, *Carbohydr. Polym.*, 2015, **126**, 199–207.
8 D. W. O'Connell, C. Birkinshaw and T. F. O'Dwyer, *J. Appl. Polym. Sci.*, 2006, **99**, 2888–2890.
9 D. W. O'Connell, C. Birkinshaw and T. F. O'Dwyer, *J. Chem. Technol. Biotechnol.*, 2006, **81**, 1820–1831.
10 M. Labet and W. Thielemans, *Polym. Chem.*, 2012, **3**, 679–684.
11 R. P. Swatloski, S. K. Spear, J. D. Holbrey and R. D. Rogers, *J. Am. Chem. Soc.*, 2002, **18**, 4974–4975.
12 G. A. Marson and O. A. ElSeoud, *J. Appl. Polym. Sci.*, 1999, **24**(6), 1355.
13 J. Wu, J. Zhang, H. Zhang, J. S. He, Q. Ren and M. L. Guo, *Biomacromolecules*, 2004, **5**, 266–275.
14 Y. Hao, J. Peng, J. Q. Li, M. L. Zhai and G. S. Wei, *Carbohydr. Polym.*, 2009, **77**, 779–792.
15 C. H. Yan, J. M. Zhang, Y. X. Lv, J. Yu, J. Wu, J. Zhang and J. S. He, *Biomacromolecules*, 2009, **10**(8), 2013–2018.
16 Y. Z. Guo, X. H. Wang, Z. G. Shen, X. C. Shu and R. C. Sun, *Carbohydr. Polym.*, 2003, **92**, 77–89.
17 Y. Zhang, X. D. Li, H. F. Li, M. E. Gibril, K. Q. Han and M. H. Yu, *RSC Adv.*, 2013, **3**, 11732–11737.
18 J. Zhu, W. T. Wang, X. L. Wang, B. Li and Y. Z. Wang, *Carbohydr. Polym.*, 2009, **76**, 139–150.
19 C. X. Lin, H. Y. Zhan, M. H. Liu, Y. Habibi, S. Y. Fu and L. A. Lucia, *J. Appl. Polym. Sci.*, 2013, **201**, 4840–4850.
20 Z. K. Wang, Y. Q. Zhang, F. Jiang, H. G. Fang and Z. G. Wang, *Polym. Chem.*, 2014, **5**, 3379.
21 C. X. Lin, H. Y. Zhan and M. H. Liu, *Langmuir*, 2009, **17**, 10116–10119.
22 C. X. Lin, S. Qiao, D. H. Liu and M. H. Liu, *Chin. J. Chem.*, 2013, **31**, 1551–1556.
23 D. H. Kumar Reddy, K. Seshaiah, A. V. R. Reddy and S. M. Lee, *Carbohydr. Polym.*, 2012, **88**(3), 1077–1086.
24 X. L. Yu, D. J. Kang, Y. Y. Hu, S. R. Tong, *et al.*, *RSC Adv.*, 2014, **4**, 31362–31369.
25 Y. Habibi, A.-L. Goffin, N. Schiltz, E. Duquesne, P. Dubois and A. Dufresne, *J. Mater. Chem.*, 2008, **18**(41), 5002–5016.
26 W. Z. Yuan, J. Y. Yuan, F. B. Zhang and X. M. Xie, *Biomacromolecules*, 2007, **8**, 1101–1123.
27 K. P. Mansikkam, M. Lahtinen and K. Rissanen, *Cellulose*, 2005, **12**(3), 233–246.
28 S. Raymond and H. Chanzy, *Macromolecules*, 1995, **28**(24), 8422–8428.
29 T. W. Weber and R. K. Chakraborty, *AIChE J.*, 1974, **20**, 228–235.
30 Y. C. Tang, Q. L. Ma, Y. F. Luo, L. Zhai, Y. J. Che and F. J. Meng, *J. Appl. Polym. Sci.*, 2013, **203**, 1799–1809.
31 O. Hamdaoui and E. Naffrechoux, *J. Hazard. Mater.*, 2007, **147**, 381–389.
32 M. M. Montazer-Rahmati, P. Rabbani, A. Abdolali and A. R. Keshtkar, *J. Hazard. Mater.*, 2007, **185**(1), 401–407.
33 R. A. Anayurt, A. Sari and M. Tuzen, *Chem. Eng. J.*, 2009, **151**(1–3), 255–263.
34 S. N. Milmile, J. V. Pande, S. Karmakar, A. Bansiwal, T. Chakrabarti and R. B. Biniwale, *Desalination*, 2011, **276**(1–3), 38–50.
35 M. I. Temkin, *Zh. Fiz. Khim.*, 1941, **15**, 2961–2964.
36 T. Hajeeth, K. Vijayalakshmi, T. Gomathi and P. N. Sudha, *Int. J. Biol. Macromol.*, 2013, **62**, 59–72.
37 N. Aoki, K. Fukushima, H. Kurakata, M. Sakamoto and K. Furuhata, *React. Funct. Polym.*, 1999, **42**(3), 223–231.